

An acoustic microscopy technique reveals hidden morphological defenses in *Daphnia*

Christian Laforsch^{*†}, Wilfred Ngwa[‡], Wolfgang Grill[‡], and Ralph Tollrian^{*}

^{*}Department of Biological Sciences, Institute of Environmental and Natural Sciences, Lancaster University, Lancaster LA1 4YQ, United Kingdom; and [‡]University of Leipzig, Institute for Experimental Physics II, Linnéstrasse 5, 04103 Leipzig, Germany

Edited by May R. Berenbaum, University of Illinois at Urbana-Champaign, Urbana, IL, and approved September 30, 2004 (received for review July 7, 2004)

Inducible defenses are common strategies for coping with the selective force of predation in heterogeneous environments. In recent years the conspicuous and often dramatic morphological plasticity of several waterflea species of the genus *Daphnia* have been found to be inducible defenses activated by chemical cues released by predators. However, the exact defensive mechanisms remained mysterious. Because even some minute morphological alterations proved to be protective against predatory invertebrates, it has been suggested that the visible morphological changes are only the tip of the iceberg of the entire protective mechanisms. Here we applied a method of ultrasonic microscopy with vector contrast at 1.2 GHz to probe hidden morphological defenses. We found that induction with predator kairomones increases the stability of the carapace in two *Daphnia* species up to 350%. This morphological plasticity provides a major advantage for the induced morphs during predation because predatory invertebrates need to crush or puncture the carapace of their prey to consume them. Our ultrastructural analyses revealed that the internal architecture of the carapace ensures maximal rigidity with minimal material investment. Our results uncover hidden morphological plasticity and suggest a reconsideration of former classification systems in defended and undefended genotypes in *Daphnia* and possibly in other prey organisms as well.

Predation is a decisive factor of natural selection (1, 2). In both animals and plants, different defensive mechanisms have evolved. Inducible defenses have been frequently reported in almost every biological community (3). They enable prey organisms to express a particular defense only if a reliable cue for a future attack is present (4–8). Thereby, the organisms can minimize costs affiliated with the formation of a defense when predation risk is low. Several *Daphnia* species form inducible defenses in response to chemical cues from predators (kairomones) (9–11). Although some induced morphological changes in *Daphnia* are extremely tiny, they have been shown to reduce predator caused mortality (Fig. 1a) (11). Despite intense research, the exact defensive mechanisms have remained unresolved. Because many predatory invertebrates possess specialized mouthparts (Fig. 1b), the “anti-lock-and-key hypothesis” had been formulated (12) to state that the morphological features render the prey incompatible to the mouthparts of the predator. Other researchers (13) suggested that the visible morphological changes are just the tip of the iceberg of protection and that hidden changes may be partly responsible for the defensive effects. Furthermore, it has been shown that several traits may act synergistically to form a defense (10). Similarly, changes in life history and behavior (14, 15) can act as defenses. In contrast to the more obvious traits, little work has been done on the armor of the animals, the carapace (16). We aimed to search for increased stability of the armor of *Daphnia pulex* and *Daphnia cucullata* exposed to water-soluble chemicals released by the predacious phantom midge larvae. We applied in this study the method of ultrasonic microscopy with vector contrast at 1.2 GHz, to solve ecologically relevant questions.

Acoustic microscopy allows to image, with microscopic resolution, the interaction of acoustic waves with the mechanical

properties of a sample. A diffraction-limited focus is formed on the sample by a lens, functions to transmit monochromatic acoustical signal and the receiving of the reflected signal. The final image is formed by scanning the lens mechanically in a plane parallel to the sample surface. The acoustic wave is modulated by the surface of the sample, and the reflected waves contain the specific information. Detailed theory is available to relate the elastic (mechanical) properties of the surface to the contrast, and this enables informed interpretation of the acoustic images to be made (17). This modus operandi provides excellent possibilities for probing mechanical properties of biological specimens, e.g., cells and cell compounds (18, 19). Crucial advantages of acoustic microscopy are that it is nondestructive and the results are not altered by specific preparation methods, such as embedding or sectioning. Furthermore, phase-sensitive acoustic microscopy, which is used in this study, presents singular advantages over conventional scanning acoustic microscopy. The 3D scanning permits the acquisition of 3D amplitude and phase images concomitantly (20). Judicious choices of focal positions can be made to optimize acoustic signals from planes of interest, because the technique is confocal and employs time-gating. The phase images contain additional sample information and allow for numerous image processing possibilities not possible with scanning acoustic microscopy. From the 3D images, the amplitude of the signal reflected under focal conditions can be determined, and the surface topography of the sample can be derived and corrected for tilt from the simultaneously acquired phase image with nanometer resolution.

Methods

Induction Experiments. Single clones of *D. pulex* and *D. cucullata* were used for our experiments. The laboratory-cultured animals were fed at unlimited food conditions (1.5 mg of C per liter) with *Scenedesmus obliquus* daily. All experiments were conducted in the laboratory under constant conditions at 20°C and fluorescent light in a synthetic medium (21). Daphnids were age-synchronized by collecting mothers with freshly deposited eggs. The third brood of these mothers was put in the experimental jars.

Then 50 *D. pulex* were placed separately into each chamber of tissue plates containing 5 ml of artificial medium. Predator kairomone from *Chaoborus flavicans* (15 larvae per liter) was added daily into each of the 25 chambers of the induction treatment. The rest of the chambers served as control. After the release of the first brood, the mothers were removed from the chambers. The young daphnids underwent one more molt before they were fixed in 70% EtOH (pro analysis) in the second juvenile stage. During this life stage, *D. pulex* generates most pronounced neck-teeth. Predator-kairomone-induced daphnids were checked under a microscope for neck-teeth induction. Fifteen *D. cucullata* were introduced into each of 10 glass vessels

This paper was submitted directly (Track II) to the PNAS office.

[†]To whom correspondence should be addressed. E-mail: c.laforsch@lancaster.ac.uk.

© 2004 by The National Academy of Sciences of the USA

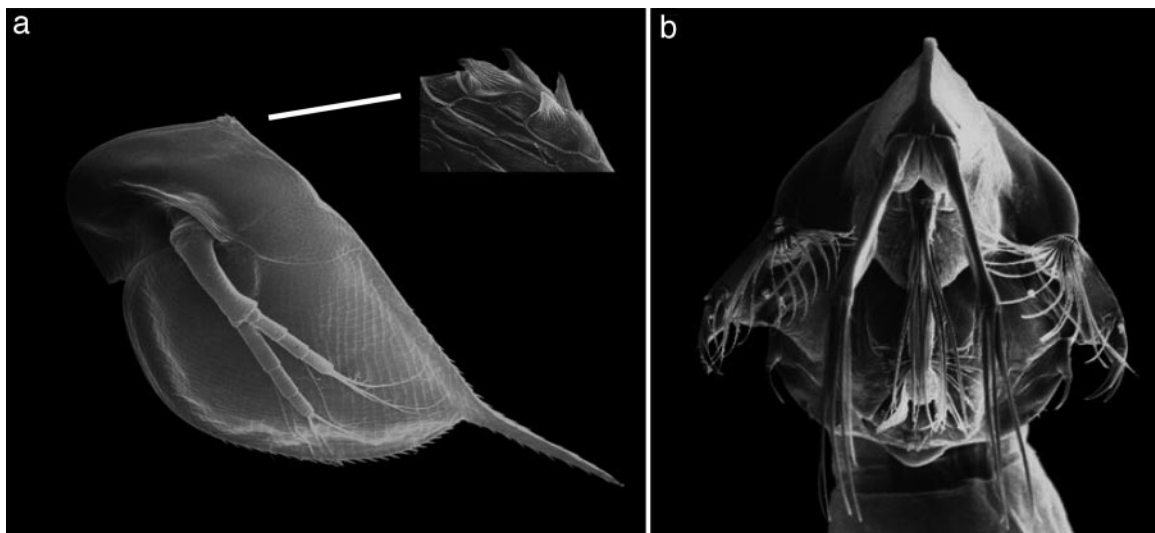


Fig. 1. Scanning electron microscopy. (a) Scanning electron micrograph of the second juvenile stage of a predator-exposed *D. pulex* (27). The development of neck-teeth was speculated to be the tip of an iceberg of a defense. (b) Scanning electron micrograph of an expanded feeding basket of *C. flavicans*.

containing 1 liter of artificial medium. Helmet elongation of *D. cucullata* was induced by using small-scale turbulence (22) and predator kairomone from *C. flavicans* (15 larvae per liter) simultaneously to ensure a strong induction effect. Five vessels served as the control. Adult daphnids were removed after the birth of the first generation. Daphnids were fixed in 70% EtOH (pro analysis) and stored in 50-ml glass jars after having reached maturity.

Acoustic Microscopy. Before ultrasonic microscopy, the daphnids were also fixed with 70% methanol for 1 h on ice. Afterward, the daphnids were washed three times in artificial medium. A single randomly selected *Daphnia* was placed with a Pasteur pipette onto a glass cover slide (ϕ , 10 mm). A small drop of histoacryl was placed with a dissecting needle onto the dry surface of the cover slide, because the glue polymerizes when getting in contact with water. The daphnid was attached to the glue by gently moving its body (still covered with medium) into the drop by using an eyelash fixed upon a toothpick. The cover slide was mounted with double-stick tape onto the scanner.

The transducer of the phase-sensitive acoustic microscope (23), acting in this case like a light-sensitive receptor and coherent detector, converts the signal reflected from the sample to an electromagnetic signal. The signal is processed in a quadrature-detection scheme (23), resulting in two low-frequency signals, which are both digitized and stored (with 12-bit conversion) for each pixel of the image by a two-channel image-processing unit. The amplitude and phases are calculated point-by-point from these data, using Pythagoras' theorem and the inverse tangent. The amplitude of the reflected pulse is proportional to the acoustic reflectivity of the object at the point being investigated. The image slices obtained by 3D scanning were used for deriving a maximum-amplitude image representing the amplitude as being at the focus (Fig. 2b). In this study, the reflectivity R_{dB} in decibels is given by: $R_{dB} = 20 \log(x/k)$. The x is the average in focus amplitude of the reflected signal from a region of interest on the carapace. The constant $k = 2,896.3$ is the maximum amplitude obtainable from the two-frame, 12-bit data acquisition. At 1.2 GHz, the resolution is $\approx 1 \mu\text{m}$. The coupling medium was composed of one part ultra-pure water, two parts tap water, 10 ml/liter salt medium for *Blepharisma*, 1.5 μl /liter sea salt solution, and 100 μl /liter SeO_2 .

Light Microscopy and Digital Data Analysis. Predator and nonpredator exposed *D. cucullata* were embedded in Durcupan, and 4- μm semithin sections were made in horizontal alignment by using a microtome. The thickness of the carapace was measured with a

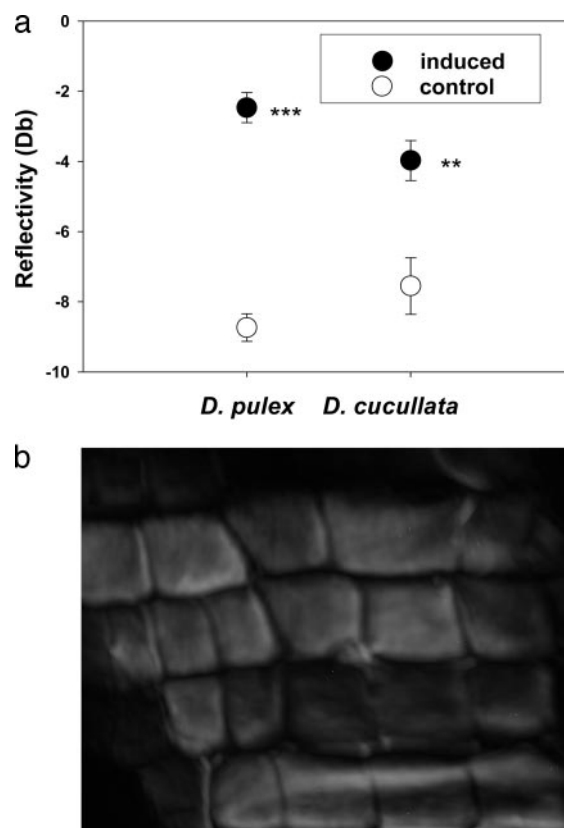


Fig. 2. Acoustic microscopy. (a) Mean reflectivity (measurement of the strength of a material) of the carapace of *D. cucullata* and *D. pulex*. Plastic responses of both *Daphnia* species were induced by water-soluble chemicals released by the predacious phantom-midge larvae. Asterisks indicate significant differences to the control (***, $P < 0.001$; **, $P < 0.01$). (b) A 1.2-GHz phase-sensitive acoustic microscopy amplitude image of the carapace of *D. pulex* ($140 \times 150 \mu\text{m}^2$).

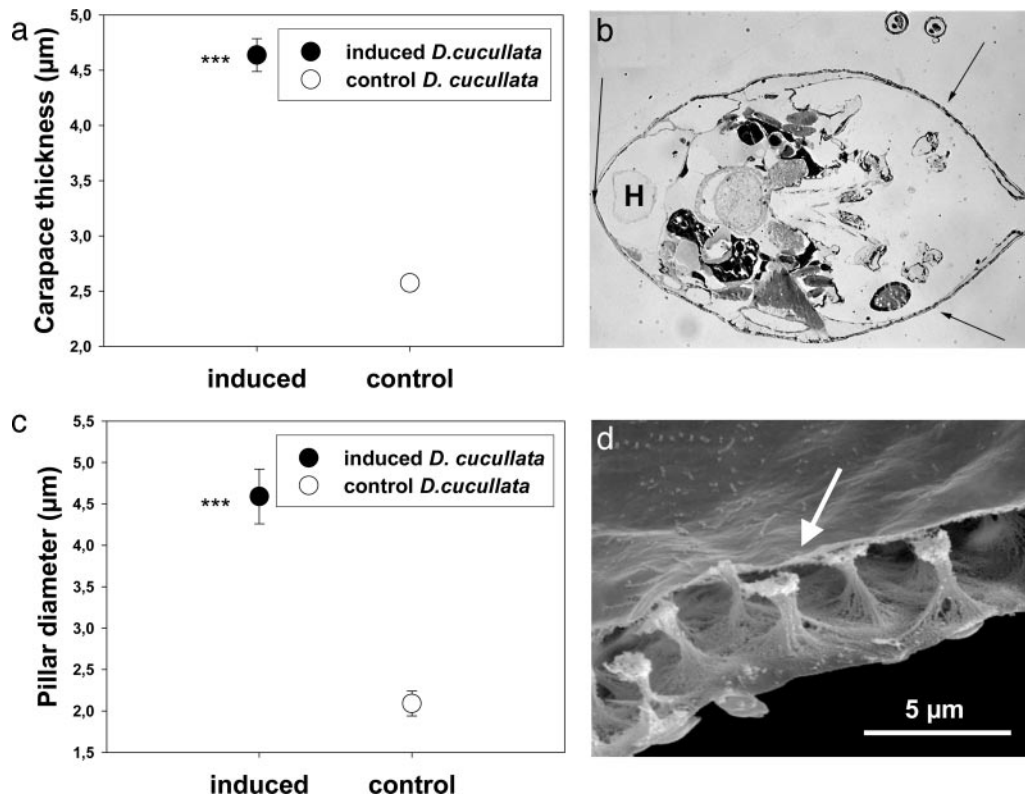


Fig. 3. Ultrastructural analysis. (a) Mean carapace thickness of *D. cucullata* exposed to chemical signals released from *C. flavicans* (induced) compared with control animals. Asterisks indicate significant differences to the control (***, $P < 0.001$). (b) Measurements were standardized by analyzing thickness of the armor at three defined points (indicated by arrows) in a semithin-section in the region of the heart (H) in each daphnid. (c) Mean pillar diameter of predator- (induced) and nonpredator-exposed (control) *D. cucullata*. Asterisks indicate significant differences to the control (***, $P < 0.001$). (d) Scanning electron micrograph showing the lightweight construction of the armor. The pillars (arrow) connect the outer and inner carapace layer.

digital image analysis system (ANALYSIS PRO, Soft Imaging System, Lakewood, CO) under a light microscope at three points of the armor in the region of the pericard (see Fig. 3b). Data of control and induced animals were compared by using *t* tests.

In the second experiment, previously fixed animals of predator- and nonpredator-induced *D. cucullata* were stained with haematoxylin. The pillar diameters were analyzed in both treatments under the light microscope by using the digital image analysis system. Exactly defined regions of interest were selected on each *Daphnia* (covering ≈ 150 pillars/*Daphnia*). Each *Daphnia* was subsequently handled as a replicate. Data were tested for normal distribution and homogeneity of variances. To compare between predator- and nonpredator-induced *Daphnia*, a nested ANOVA was then performed to test for treatment effects by using treatment as fixed factor and replicate as random factor.

Results and Discussion

For both *D. pulex* and *D. cucullata*, a phase-sensitive acoustic microscopy probe of the mechanical properties (bending strength, tensile strength, and hardness) of the carapace revealed that the mean reflectivity for the predator-kairomone-induced samples was significantly higher than in the noninduced samples (Fig. 2a; *D. pulex*: $t = 10.77$, $df = 40$, $P < 0.001$; *D. cucullata*: $t = 3.34$, $df = 27$, $P = 0.002$). Higher reflectivity is tantamount to higher acoustic impedance of the carapace. The acoustic impedance of a material is defined as the product of density and acoustic velocity of that material. It is a measure of material “hardness” and describes the ability of the material to withstand penetration by a surface contact, which in our case could be the mandibles of a predator. Acoustic impedance is important in the determination of

acoustic transmission and reflection at the interface of two materials (in this case, *Daphnia* carapace and the coupling medium). In addition to amplitude, the reflection from a given interface also has a positive or negative polarity, i.e., whether the acoustic impedance increases (positive) or decreases (negative) as ultrasound crosses the interface. From the phase of the reflected acoustic signal, it was determined that the polarity of the reflected signals from the carapace for both induced and noninduced samples examined was positive. In *D. pulex* reflectivity of the induced morphs was found to be on average 350% greater than that of the noninduced samples, whereas in *D. cucullata* it is doubled (Fig. 2a). This strengthening of the armor could explain the high escape efficiencies for induced specimens even after being caught by the phantom midge larvae (21, 24). Although the mandibles of the predator are rigid structures, by virtue of a more than two times harder surface it requires much more strength to penetrate the armor. Moreover, the feeding basket of *C. flavicans* (Fig. 1b) is made of fine cuticular appendages and the harder armor results in more endeavor or prevention to fold the carapace of the prey.

To reveal the structural cause of the higher stability, we conducted an ultra-structural analysis. Semithin-sections of the carapace of *D. cucullata* showed that predator-exposed animals had significantly thicker carapaces than control animals raised without chemical cues (Fig. 3a; $t = -12.5$, $df = 532$, $P < 0.001$). The carapace of *Daphnia* consists of two epidermal layers connected by small pillars (Fig. 3d). The average diameter of the pillars from *D. cucullata* exposed to predator kairomones was twice as large as in the control animals (Fig. 3c; nested ANOVA; $df = 23$, $F = 204.1$, $P < 0.001$). This result implies that a fortification of the carapace is realized with low material expen-

diture. The extensions of the pillars, which are also built of small fibers (Fig. 3d), strengthen the mechanical stability of the whole carapace but are a “lightweight” construction. The evolutionary arms race between predator and prey drives the establishment of cost saving but effective defense mechanisms. Investments in a lightweight architecture which result in a 2- to 3.5-fold increased stability, provide an enormous advantage. They guarantee an effective defense while minimizing material investment, similar to recent results from diatoms (25).

Our finding that *Daphnia* possess “hidden” defensive traits may explain the paradox that induced but seemingly undefended daphnids still reduce their vulnerability to predators, which up to now has been attributed to the existence of unknown behavioral defenses (16, 26).

Our results indicate that induced daphnids are physically better protected against mechanical challenges by strengthening

their armor. This likely provides the crucial advantage in struggling out of catching apparatus of the predator during an attack. Although our study questions the current paradigm for the defensive mechanism, the anti-lock-and-key hypothesis, it does not rule out that both effects, incompatibility with the predator mouthparts and increased mechanical stability, act synergistically. Although we have tested only the armor of two *Daphnia* species, we expect this hidden morphological plasticity to be common in *Daphnia* species threatened by small predatory invertebrates and possibly in other prey organisms. Our study highlights the auspicious opportunities of interdisciplinary projects, where new physical methods lead to new insights into biological questions.

We thank W. Gabriel for support and discussion, M. Kredler for help during experiments, Scott Stevens for linguistic improvements, and two anonymous reviewers for comments on the manuscript.

1. Sih, A., Englund, G. & Wooster, D. (1998) *Trends Ecol. Evol.* **13**, 350–355.
2. Kerfoot, W. C. & Sih, A., eds. (1987) *Predation: Direct and Indirect Impacts on Aquatic Communities* (Univ. Press of New England, Hanover, NH).
3. Tollrian, R. & Harvell, C. D., eds. (1999) *The Ecology and Evolution of Inducible Defenses* (Princeton Univ. Press, Princeton).
4. Harvell, C. D. (1984) *Science* **224**, 1357–1359.
5. Brönmark, C. & Miner, J. G. (1992) *Science* **258**, 1348–1350.
6. Van Buskirk, J., McCollum, S. A. & Werner, E. E. (1997) *Evolution (Lawrence, Kans.)* **51**, 1983–1992.
7. Agrawal, A. A., Laforsch, C. & Tollrian, R. (1999) *Nature* **401**, 60–63.
8. Leonard, G. H., Bertness, M. D. & Yund, P. O. (1999) *Ecology* **80**, 1–14.
9. Grant, J. W. G. & Bayly, I. A. E. (1981) *Limnol. Oceanogr.* **26**, 201–218.
10. Spitze, K. & Sadler, T. D. (1996) *Am. Nat.* **148**, S108–S123.
11. Tollrian, R. & Dodson, S. I. (1999) in *The Ecology and Evolution of Inducible Defenses*, eds. Tollrian, R. & Harvell, C. D. (Princeton Univ. Press, Princeton), pp. 177–202.
12. Dodson, S. I. (1974) *Limnol. Oceanogr.* **19**, 721–729.
13. Tollrian, R. (1993) *J. Plankton Res.* **15**, 1309–1318.
14. Boersma, M., Spaak, P. & De Meester, L. (1998) *Am. Nat.* **152**, 237–248.
15. De Meester, L., Weider, L. J. & Tollrian, R. (1995) *Nature* **378**, 483–485.
16. Dodson, S. I. (1984) *Ecology* **65**, 1249–1257.
17. Yu, Z. & Boseck, S. (1995) *Rev. Mod. Phys.* **67**, 863–891.
18. Kundu, T., Bereiter-Hahn, J. & Karl, I. (2000) *Biophys. J.* **78**, 2270–2279.
19. Wagner, O., Zinke, J., Dancker, P., Grill, W. & Bereiter-Hahn, J. (1999) *Biophys. J.* **76**, 2784–2796.
20. Grill, W., Hillman, K., Kim, T. J., Lenkeit, O., Ndop, J. & Schubert, M. P. (1999) *Physica B (Amsterdam, Neth.)* **263–264**, 553–558.
21. Laforsch, C. & Tollrian, R. (2004) *Ecology* **85**, 2302–2311.
22. Laforsch, C. & Tollrian, R. (2004) *J. Plankton Res.* **26**, 81–87.
23. Grill, W., Hillman, K., Würz, K.-U. & Wesner, J. (1996) in *Advances in Acoustic Microscopy*, eds. Briggs, A. & Arnold, W. (Plenum, New York), Vol. 2, pp. 167–218.
24. Spitze, K. (1992) *Am. Nat.* **139**, 229–247.
25. Hamm, C. E., Merkel, R., Springer, O., Jurkojc, P., Maier, C., Prechtel, K. & Smetacek, V. (2003) *Nature* **421**, 841–843.
26. Luning, J. (1995) *Freshwater Biol.* **34**, 523–530.
27. Laforsch, C. & Tollrian, R. (2000) *Arch. Hydrobiol.* **149**, 587–596.